

An approach to quick and easy evaluation of the dam breach flood

CHEN ZuYu^{1,2,3*}, PING ZiYi^{1,2}, WANG NaiXin³, YU Shu³ & CHEN ShuJing⁴¹ Institute of Geotechnical Engineering, Zhejiang University, Hangzhou 310027, China;² Key Laboratory of Soft Soils and Geoenvironmental Engineering of Ministry of Education, Zhejiang University, Hangzhou 310058, China;³ State Key Laboratory of Simulation and Regulation of Water Cycle in River Basin, China Institute of Water Resources and Hydropower Research, Beijing 100038, China;⁴ Department of Engineering Training, National Academy for Mayors of China, Beijing 100029, China

Received July 21, 2018; accepted September 28, 2018; published online March 21, 2019

In the context of an impending dam failure, quick evaluation of dam breach flood is necessary. Previous studies provided an approach to calculate the dam breach hydrograph using an Excel spreadsheet based on the improved soil erosion model and numerical algorithm. However, calculation of the breach lateral enlargement requires the modeling of the successive collapse of the breach banks. It is time-consuming with special training, which is difficult to provide during an emergency. This study proposes that the lateral enlargement process can be modeled using a hyperbolic relationship with sufficient accuracy. Consequently, field engineers can perform the dam breach analysis along with the sensitive study for a target case within 1 h in an Excel spreadsheet which is self-tutorial. This paper presents this easy and quick approach based on only fifteen input parameters that can be determined based on the experience. This approach can also be used for the preliminary study when a dam safety planning work is undertaken.

dam breach flood, breach lateral enlargement, hyperbolic relationship

Citation: Chen Z Y, Ping Z Y, Wang N X, et al. An approach to quick and easy evaluation of the dam breach flood. *Sci China Tech Sci*, 2019, 62: 1773–1782, <https://doi.org/10.1007/s11431-018-9367-4>

1 Introduction

Breach of man-made earthen dams, landslide dams, and tailing dams have a significant social implication because the dam breach often comes without early warning. As a part of the emergency action plan, the extent of the dam breach flood must be evaluated quickly to develop a plan for the safe evacuation of the downstream population. Over or under-estimation of the flood level could both have serious social consequences, for example, the inaccurate flood estimation resulted in the evacuation of 275000 people during the Tangjiashan Barrier Lake breach [1]. Although several analytical methods and computer programs are available for the dam breach flood evaluation [2–6], their applications are

occasionally limited due to the extensive trainings and the numerical intractability and input sensitivity.

During the past decade, the authors have improved the existing dam breach analytical method such that it is physically representative, numerically friendly and less sensitive to the input parameters [7–10]. The new method is implemented using two Excel spreadsheets [7,9]. The DB-IWHR spreadsheet performs the main hydraulic calculation, while the DBS-IWHR sheet is used to model the lateral enlargement of the breach. It has been found that DB-IWHR requires only a few input parameters and the straight-forward numerical algorithm allows almost instant calculations. However, its input on breach lateral enlargement comes from another independent program DBS-IWHR that calculates the successive collapses of the breach banks [9]. The calculation is time-consuming and requires manual operations through-

*Corresponding author (email: chenzuyu@cashq.ac.cn)

out the process. In addition, it needs time for unexperienced engineers to learn from the manual, which may not be relevant during the emergence actions.

Although simple analytical approaches based on the wedge failure mode have been proposed [2], they do not reflect the actual lateral enlargement behavior because the approaches do not adequately consider the progressive failure due to the vertical cutting of the bank toes. The method proposed by Osman and Thorne [11] tries to model this cutting process. However, it determines the critical inclination of the slip surface by setting the derivative equal to zero with respect to the cohesion c . Wang [12] argued that the cohesion is a constant parameter and could not be optimized. The critical slip surface is generally determined in the soil mechanics discipline based on its location and shape [13,14]. Developing novel empirical approach to determine the lateral enlargement with an acceptable accuracy could provide a quick and easy approach for the dam breach flood prediction.

The study presented in this paper produced empirical charts that can predict the lateral enlargement based on the shear strength parameters of the dam material using a hyperbolic relationship with sufficient accuracy. Consequently, the field engineers can finish the dam flood calculations for a target case and several parametric studies within 1 h. This paper provides a brief explanation of this simple and quick dam flood evaluation method with an emphasis on the new findings regarding the hyperbolic lateral enlargement model.

2 Hydraulics in breach flood modeling

2.1 Energy and mass conservation equation

The controlling equation in a dam breach flood calculation requires the balance of water quantity as follows:

$$CB(H-z)^{3/2} = \frac{\Delta W \Delta H}{\Delta H \Delta t} + q, \tag{1}$$

where C is the discharge coefficient of the broad-crested weir flow ranging from 1.3 to 1.7 [15], H is the water elevation in the reservoir (Figure 1), from a reference elevation H_0 [7], q is the natural inflow into the reservoir, z is the channel bed elevation and t is the time. W is the reservoir water storage and can be approximated by a parabolic equation with regressed coefficients p_1, p_2, p_3 as follows:

$$W = p_1(H-H_0)^2 + p_2(H-H_0) + p_3. \tag{2}$$

The water level generally drops at the entrance. Chen et al.

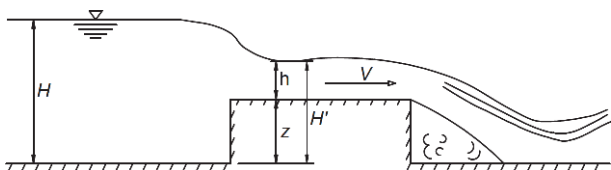


Figure 1 Flow over a broad-crested weir.

[7] introduced an empirical parameter, the water drop ratio, m , to determine the water depth behind the weir, as follows:

$$h = m(H-z). \tag{3}$$

It has been found that the calculated peak flow is not sensitive to m , which varies between 0.5 and 0.8.

2.1 Hyperbolic soil erosion model

Chen et al. [7] noted that the linear and power relationships models used in various dam breach analysis software have limitations of the sensitive calculated peak flows due to the input parameters [7,10]. Consequently, they proposed the following hyperbolic relationship for the back analysis for the Tangjiashan Barrier Lake (Figure 2):

$$z = \Phi(\tau) = \frac{v}{a+bv}, \tag{4}$$

where v is the shear stress with reference to its critical component τ_c which can be given by the following equation:

$$v = k(\tau - \tau_c), \tag{5}$$

with a unit of Pa for τ and 10^{-3} mm/s for z , k is the unit conversion factor and is generally 100. The hyperbolic curve asymptotes to $1/b$ as v approaches infinity, while $1/a$ represents the tangent of this curve at $v=0$.

$1/a$ is approximately equal to the coefficient describing the linear relationship when the shear stress is small. The asymptote $1/b$ represents the maximum possible erosion rate, suggesting that the erosion rate would yield when the shear stress is sufficiently large. The asymptote $1/b$ would prevent the calculated erosion rate from becoming too large during the high flow velocity, resulting in the extra peak flow. The authors performed laboratory experiments and confirmed the effectiveness of this model [16]. Based on the experimental outcomes and several case study results [17], this paper proposes the ranges for the parameters a and b for different soil types (Table 1) to be used by the field engineers during the emergency when the detailed laboratory tests on soil erosion are not possible.

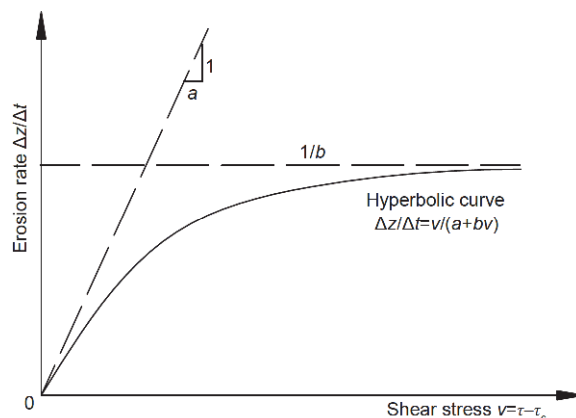


Figure 2 Relationship between soil erosion rate and shear stress in the hyperbolic model.

Table 1 Suggested values for a and b for preliminary studies

Erodibility	Soil materials	a	b
Very high	Fine sand, Non-plastic silt	1.0–1.1	0.0001–0.0003
High	Medium sand, Low plasticity silt	1.0–1.1	0.0003–0.0005
Medium	Jointed rock (spacing <30 mm), Fine gravel, Coarse sand, High plasticity silt, Low plasticity clay, All fissured clays	1.1–1.2	0.0005–0.0007
Low	Jointed rock (30–150 mm spacing), cobbles, Coarse gravel, High plasticity clay	1.1–1.2	0.0007–0.001
Very low	Jointed rock (150–1500 mm spacing), Riprap	1.2–1.5	0.001–0.01
Non-erosive	Intake rock, Jointed rock (spacing >1500 mm)	1.2–1.5	0.01–0.1

3 Geomechanics for lateral enlargement modeling

3.1 Modeling the breach enlargement

In the geotechnical context, Chen et al. [7] highlighted that the wedge slide method commonly used to model the widening of the discharge channel [3,4] require a more representative approach that employs a circular slip surface using the Bishop's simplified method [18]. The DBS-IWHR spreadsheet developed by Wang et al. [9] has been used to calculate the minimum factor of safety and the critical depth of toe cutting. In the procedure, the factor of safety F is repeatedly calculated to find the critical depth of toe cutting Δz which makes the minimum factor of safety $F_m=1$. The stepped bank corruptions are believed to occur, with the characteristic features shown in Table 2. Figure 3(a) presents a model for the successive collapse of the breach banks due to the vertical toe cutting by soil erosions. The associated material properties used in this model are as follows: unit weight $\gamma=16 \text{ kN/m}^3$, cohesion $c=15 \text{ kPa}$, and friction angle $\phi=37^\circ$. To simplify the approach for numerical convenience,

Table 2 β and $\Delta\beta$ associated with the toe cutting depth Δz

Step	Δz (m)	β ($^\circ$)	$\Delta\beta$ ($^\circ$)
1	1.500	123.43	6.93
2	3.052	125.80	9.30
3	4.573	128.93	12.43
4	6.236	130.78	14.28
5	8.232	130.54	14.04
6	10.141	131.58	15.08
7	11.921	133.96	17.46
8	13.954	134.94	18.44
9	15.686	138.31	21.81
10	18.559	136.46	19.96
11	20.991	138.22	21.72
12	23.764	138.86	22.36
13	26.899	138.92	22.42
14	30.448	138.34	21.84
15	33.014	141.49	24.99

Wang et al. [9] suggested to approximate the circular arcs to the straight lines by assuming the inclination β as the average of the inclinations of the chord and the tangent of the circles at the toe (Figure 3(b)). The β values associated with the toe cutting depth Δz are given in Table 2. It should be emphasized that the simplification remains its physical implication of circular slip surfaces.

DB-IWHR determines the intermediate values of β by linear interpolation as follows:

$$\beta = \beta_0 + \frac{z_0 - z}{z_0 - z_{\text{end}}}(\beta_{\text{end}} - \beta_0), \quad (6)$$

where z is the elevation of the eroded bed. The subscripts '0' and 'end' refer to the values at the beginning and the end, respectively.

The initial width, B_0 , may be determined based on the inflow of the reservoir as shown below [7]:

$$B_0 = \frac{C^2 q_{\text{in}}}{m^3 V_c^3}, \quad (7)$$

where q_{in} and V_c are the inflow and incipient flow velocity at the channel at the onset of the breach, respectively. B_0 can also be determined based on the experience of the practitioners followed by the sensitivity analysis. During the emergency actions for the barrier lakes, B_0 could sometimes be the width of an existing flood release channel. The Excel spreadsheet, DBS-IWHR, can be used for the calculations.

3.2 Empirical approach to modeling the progressive lateral enlargement

Although a computer program is available to calculate the progressive collapse process, it is time-consuming, inconvenient, and unsuitable for the inexperienced engineers, who would require to quickly evaluate the breach flood. Hence, it is helpful to identify an empirical approach to determine the slope inclination, β , at a collapse step based on its elevation z .

3.2.1 Evaluation of z_0 and β_0

Assuming that the breach starts in a channel with a vertical bank (Figure 4), the active earth pressure P_a applied on the vertical face is

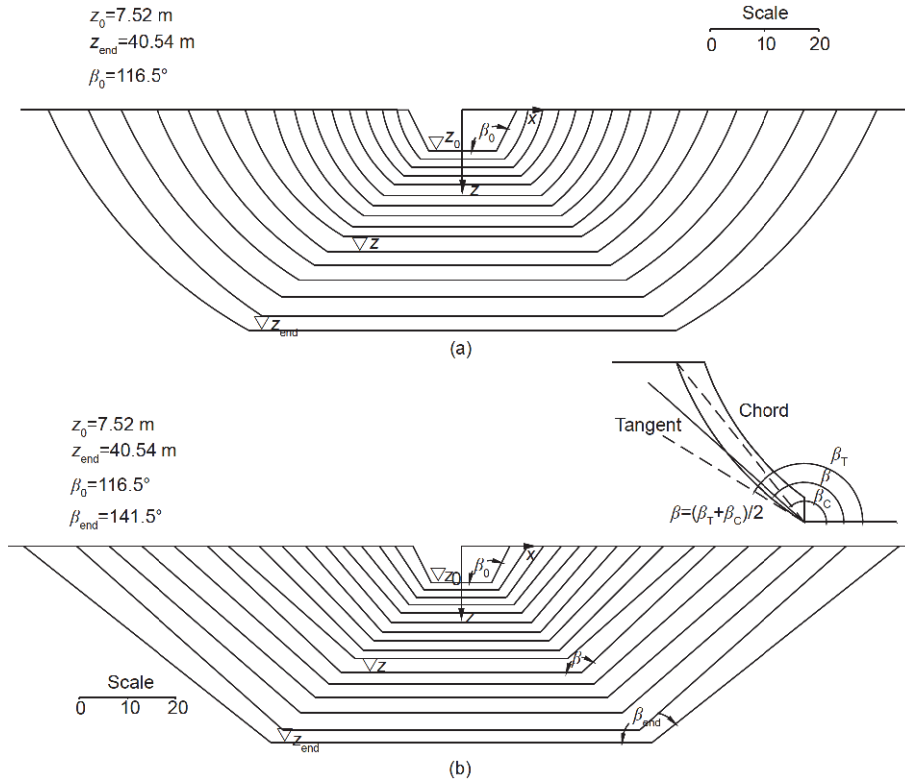


Figure 3 Modeling the lateral enlargement. (a) Circular slip surfaces; (b) straight line simplifications.

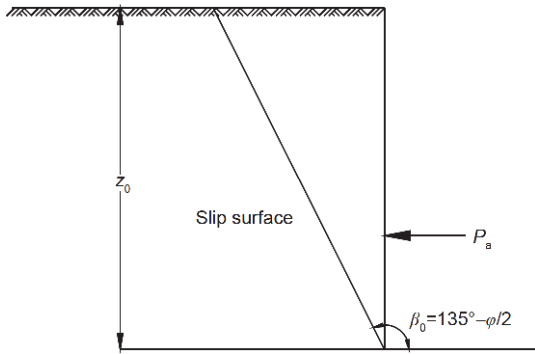


Figure 4 Cative earth pressure applied on a vertical wall.

$$P_a = \frac{1}{2} \gamma z_0^2 K_a - 2cz_0 \sqrt{K_a}, \tag{8}$$

where

$$K_a = \frac{1}{2} \tan^2(\pi/4 - \varphi/2), \tag{9}$$

where c and φ are cohesion and friction angle of the material, respectively. The critical height of the vertical face at the dam crest, which makes P_a equal zero, is then obtained using the following formula:

$$z_0 = \frac{4c}{\gamma \tan(\pi/4 - \varphi/2)}. \tag{10}$$

The slip surface is a straight line inclined at an angle of $3\pi/4 - \varphi/2$ to the horizontal, according to the Column's theory.

$$\beta_0 = 3\pi/4 - \varphi/2. \tag{11}$$

3.2.2 Evaluation of β as a function of z

Figure 5 depicts the relationship between $\Delta\beta$ and Δz from the data in Table 2. It appears that a hyperbolic relationship may exist.

$$\Delta\beta = \frac{\Delta z}{m_1 + m_2 \Delta z}, \tag{12}$$

where $1/m_1$ and $1/m_2$ represent the initial tangent and asymptote of the curve, respectively. Eq. (12) could be rearranged to eq. (13) to verify the relationship.

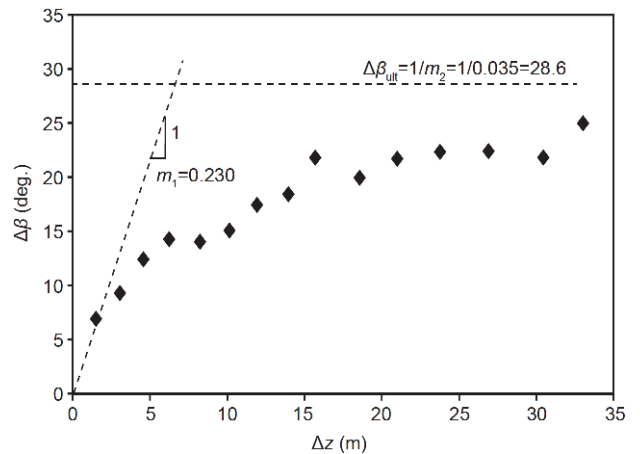


Figure 5 Hyperbolic relationship between $\Delta\beta$ and Δz by Eq. (12).

$$\frac{\Delta z}{\Delta \beta} = m_1 + m_2 \Delta z. \tag{13}$$

The relationship between $\Delta\beta$ and Δz as listed in Table 2 can be redrawn following eq. (13) as shown in Figure 6. Accordingly, the relationship is linear with m_1 of 0.230 and m_2 of 0.035, and a regression coefficient (R^2) of 0.979, demonstrating the existence of the hyperbolic relationship. It should be noted that m_1 and m_2 depend on the units of $\Delta\beta$ ($^\circ$) and Δz (m) because of the empirical approach.

Following the same procedures, it is possible to find m_1 and m_2 for different values c , $\tan\phi$ associated with $\gamma=16 \text{ kN/m}^3$ as shown in Table 3. Accordingly, the following conclusions can be made:

(1) For a given value of ϕ , m_2 does not vary significantly. For example, m_2 remains approximately at 0.033 for different c values at $\phi=37^\circ$ (Table 3). The slight deviation in the third decimal place can be attributed to the computational error.

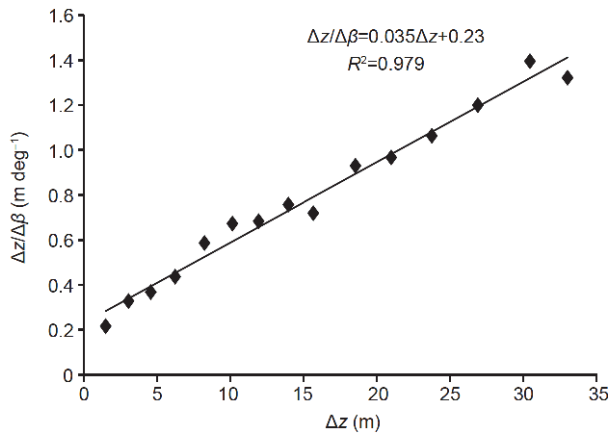


Figure 6 Hyperbolic relationship between $\Delta\beta$ and Δz by eq. (13).

The regression line in Figure 7 could be used as an empirical approach to determine m_2 based on $\tan\phi$.

(2) The contours of equal m_1 can be regressed as the functions of c and $\tan\phi$ (Figure 8), which can be used to empirically determine m_1 .

Similar relationships can be established for $\gamma=22 \text{ kN/m}^3$ (Figures 9 and 10). For material with an arbitrary γ , interpolations based on these two sets of charts would be sufficiently accurate to determine m_1 and m_2 .

For the calculation, the new version of Excel spreadsheet, DB-IWHR-2018, automatically does the interpolation based on the input values of c , ϕ and γ .

4 Solution algorithm and validation

4.1 Improved numerical algorithm

Chen et al. [7,9] provided a detailed description of the improved numerical algorithm for calculating the breach hy-

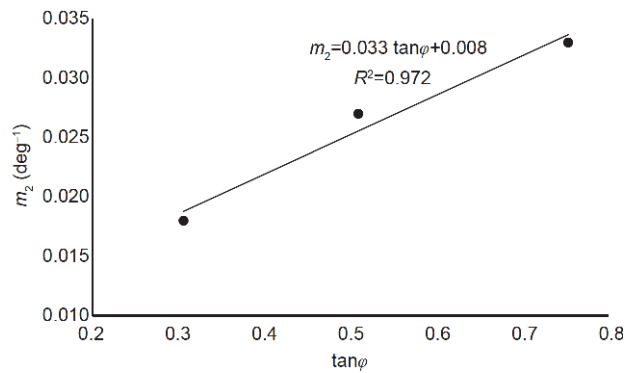


Figure 7 Empirical linear relationship between ϕ and m_2 , $\gamma=16 \text{ kN/m}^3$.

Table 3 m_1 and m_2 associated with different shear strength parameters

ϕ ($^\circ$)	c (kPa)	z_0 (m)	β_0 ($^\circ$)	m_1 (deg^{-1})	m_2 (m°)
37	15	50.142	116.5	0.230	0.035
	25	37.607	116.5	0.545	0.032
	50	25.071	116.5	0.896	0.033
	75	12.536	116.5	1.307	0.03
	100	7.521	116.5	1.504	0.033
27	15	40.796	121.5	0.128	0.028
	25	30.597	121.5	0.317	0.024
	50	20.398	121.5	0.417	0.029
	75	10.199	121.5	0.645	0.027
	100	6.119	121.5	0.781	0.028
17	15	33.786	126.5	0.107	0.016
	25	25.339	126.5	0.162	0.017
	50	16.893	126.5	0.312	0.018
	75	8.446	126.5	0.432	0.019
	100	5.068	126.5	0.607	0.018

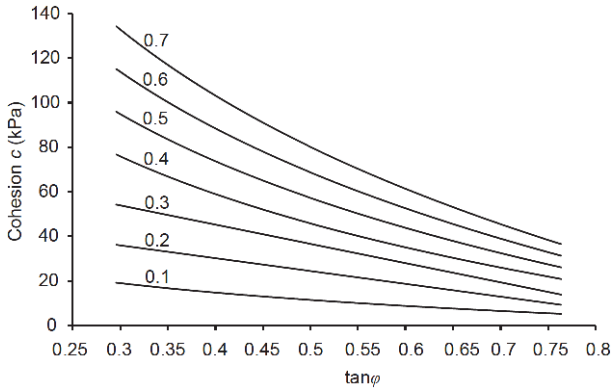


Figure 8 Empirical chart for contours of equal m_1 (deg^{-1}) based on $\tan\phi$ and c , $\gamma = 16 \text{ kN/m}^3$.

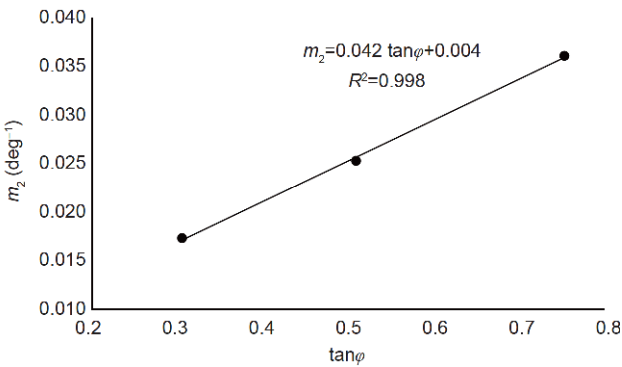


Figure 9 Empirical linear relationship between ϕ and m_2 , $\gamma = 22 \text{ kN/m}^3$.

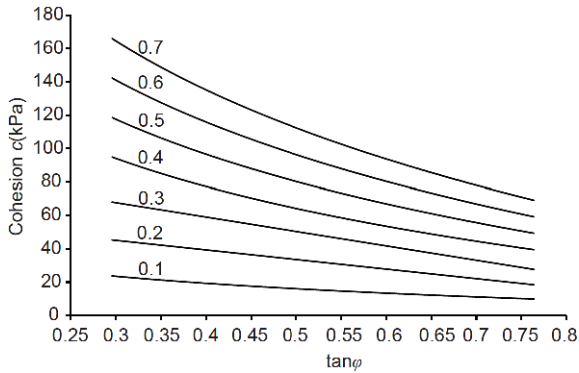


Figure 10 Empirical chart for contours of equal m_1 based on $\tan\phi$ and c , $\gamma = 22 \text{ kN/m}^3$.

drograph. They proposed the new technique that performs the integration based on a velocity increment and linearizes the governing equations for the straightforward calculation. The Excel spreadsheet, DB-IWHR, could be a simple tool for users to implement this algorithm. Figure 11 is the flowchart for the new lateral enlargement model described in this paper. This procedure is recommended on most cases. As evident in Table 4, fifteen geographical, hydraulic and geotechnical parameters are required to execute the model and they can be easily obtained in the profession for the pre-

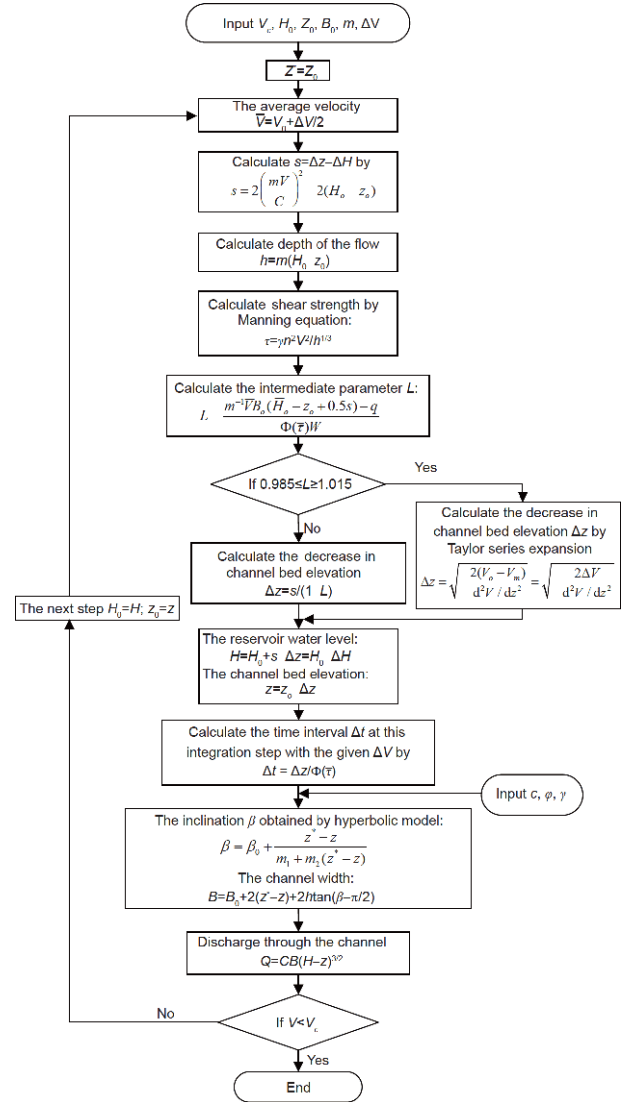


Figure 11 Flowchart for the improved numerical method (refer to [7] for undefined symbols and equations in this chart).

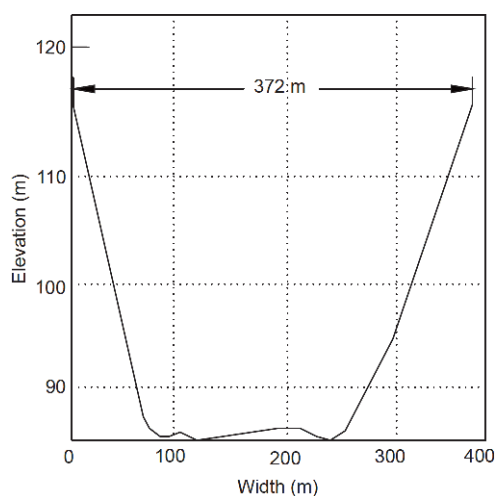
liminary study.

4.2 Illustration

This illustration analyzes the catastrophic Banqiao dam breach failure due to heavy rainfall in 1975 in Honan Province, China. The dam was 21.5 m high and 1700 m long with a crest width of 8 m. The upstream slopes was 1:3 to 1:6 (vertical:horizontal), while that of the downstream is 1:2.5 to 1:6. Due to an extremely heavy storm caused by typhoon, the majority of the Zhumadian district encountered more than 1000 mm rainfall in 3 d, developing a peak discharge of 13000 m³/s at the Ru River. Ru and Niu [19] documented the information regarding the hydrology, meteorology, and characteristic features of this overtopping failure. The measured profile of the breach (Figure 12) indicates that the breach width was 372 m at the dam crest. Zhong et al. [20]

Table 4 Input parameters for DB-IWHR

Area	Item	Symbol	Equation No.	Default	Remarks
Geography	Reservoir storage	p_1, p_2, p_3, H_0	(2)		Can be obtained either from historical records or quick survey
	Natural inflow	q	(1)		
Hydraulics	Broad-crested weir coefficient	C	(1)	1.42	Can be followed by sensitivity analysis
	Water drop coefficient	m	(3)	0.8	Can be followed by sensitivity analysis
	Incipient velocity	V_c	(4)		Many empirical suggestions are available, e.g., Briaud [17]
	Soil erosion	a, b	(4)	Table 1	(Refer to Table 1)
Geotechnique	Initial breach width and elevation	B_0, z_0			Based on inflow q or other approaches (Section 2.2)
	Material property	γ, c, φ			Can be obtained based on experience or some quick and simple tests

**Figure 12** Measured profile of the breach.

performed an independent back analysis and summarized the main features of the earth core dam. The inputs to the DB-IWHR sheet are shown in Table 5. Figure 13 depicts the outcomes.

Figure 14 shows the breach flow discharge and width associated with time, respectively. Table 6 compares the cal-

culated results against the measured values [19].

4.3 Validations

The results obtained from the original approach proposed by Wang et al. [9] using the stepped failures were compared against that of the empirical hyperbolic model approached proposed in this study. Three well-documented reports [9,10] published previously were reanalyzed. Table 7 summarizes the input for the Yigong, Xiaogangjian and Yibadao barrier lakes and Table 8 compares the results obtained by the original stepped failure mode and the new approach proposed in this study. According to Table 8, the results from both approaches are almost identical.

5 Conclusions

Rapid evaluation of the earthen dam breach flood is required during the emergency. This study found that the lateral enlargement evaluation can be reasonably modeled by a hyperbolic relationship and can complement the straightforward calculation of the breach hydrograph using an Excel

Table 5 Inputs for Banqiao dam reach analysis

Categories	Item	Parameter	Input	Remarks
Geography	Reservoir storage	p_1, p_2, p_3, H_0	1.99, -30.68, 187.17	Adapted from [20]
	Initial reservoir water level	H_0	117.94 m	
	Natural inflow	q	5000 m ³ /s	
Hydraulics	Broad-crested weir coefficient	C	1.42	Default value
	Water drop coefficient	m	0.8	Default value
	Incipient velocity	V_c	2.4 m/s	Adapted from [20]
	Soil erosion	a, b	1.0, 0.0003	From Table 1
Geotechnique	Material property	γ, c, φ	16 kN/m ³ , 30 kPa, 25°	Adapted from [20]
	Lateral enlargement coefficient	m_1, m_2	0.27, 0.02	Determined by Figures 7 and 8
	Initial channel bed elevation	z_0	115.79 m	Adapted from [20]

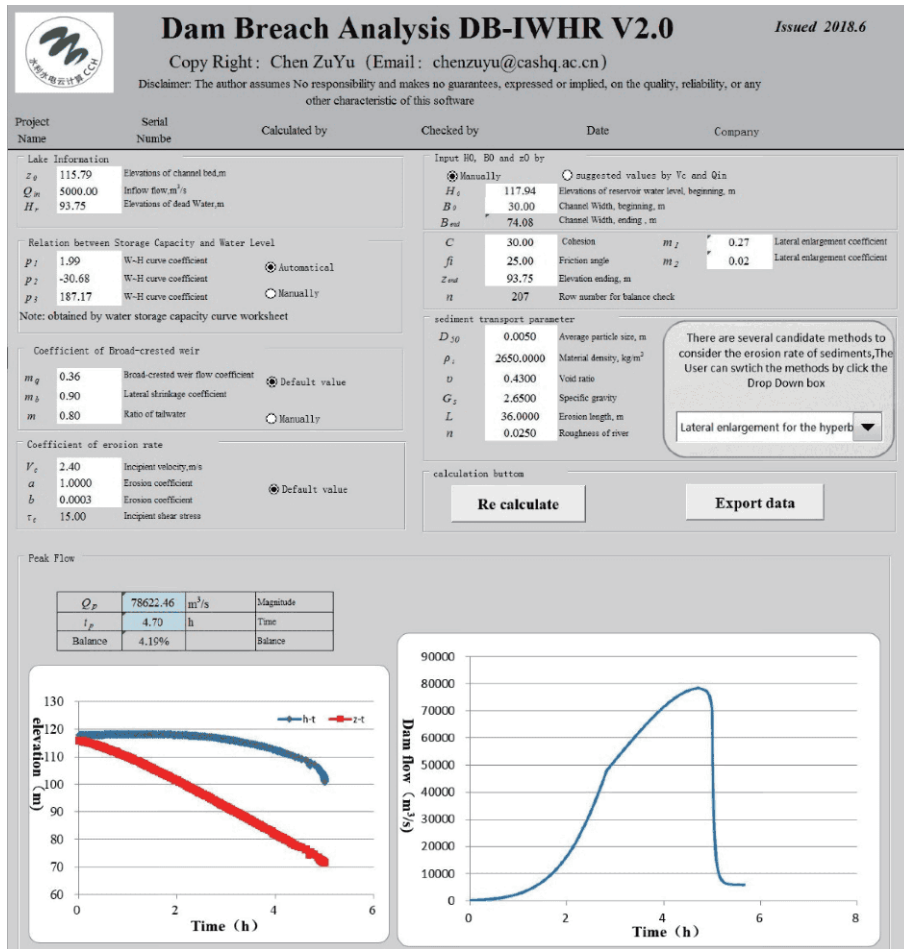


Figure 13 (Color online) Excel spreadsheet calculating the Banqiao dam hydrograph.

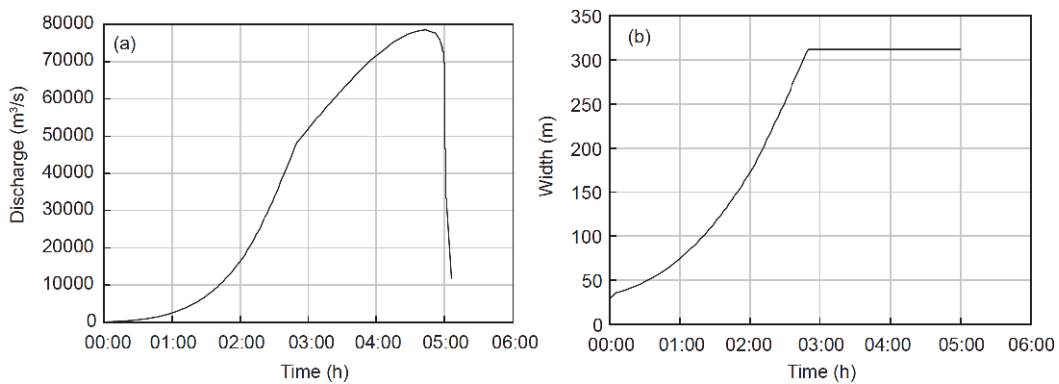


Figure 14 Discharge versus time (a) and breach width versus time (b) for the Banqiao dam breach.

Table 6 Comparison between calculated and the measured results

Parameter	Symbol (unit)	Calculated results	Measured data
Peak flow	Q_p (m^3/s)	78622	78100
Time at peak	t_p (h)	4.70	3.5
Average breach width	B_{avg} (m)	311	291

Table 7 Input of the three cases for validation

Categories	Parameters	Yigong [9]	Xiaogangjian [10]	Yibadiao [10]
Geography	p_1, p_2, p_3, H_0	0.31, 16.28, -121.78, 2262.82	0.01, -0.53, 9.54, 844.57	0.0029, 0.098, -0.58, 762.57
	q	859 m ³ /s	15 m ³ /s	Upstream dam breach flood
	H_0	2262.82 m	844.57 m	
Hydraulics	C	1.42	1.42	1.42
	m	0.8	0.8	0.8
	V_c	2 m/s	2.7 m/s	2.7 m/s
	a, b	0.3, 0.00038	0.2, 0.0002	0.2, 0.0002
	γ, c, φ	18.5 kN/m ³ , 13 kPa, 37°	18.5 kN/m ³ , 41.6 kPa, 19°	18.5 kN/m ³ , 41.6 kPa, 19°
Lateral enlargement for the hyperbolic model	m_1, m_2	0.2, 0.03	0.25, 0.02	0.25, 0.02
	B_0	5 m	30 m	15 m
Lateral enlargement for the stepped failure	$\beta_0, \beta_{\text{end}}$	119°, 145°	129°, 170°	134°, 157°
	z_0, z_{end}	2261 m, 2210 m	842 m, 813 m	760 m, 752 m

Table 8 Comparisons between both approaches^{a)}

Parameter	Symbol (unit)	Mode	Yigong		Xiaogangjian		Yibadiao	
			Calculated	Measured	Calculated	Measured	Calculated	Measured
Peak flow	Q_p (m ³ /s)	Stepped failure	106062	94013	2251.47	–	3330	3950
		Hyperbolic	102437		2272.86		3329	
Time at peak	t_p (h)	Stepped failure	6.77	6.17	0.93	0.45	1.02	0.45
		Hyperbolic	6.56		0.91		1.00	
Breach width	B_{end} (m)	Stepped failure	424.0	430	106.6	122	64.6	57
		Hyperbolic	420.0		100.4		60.7	

a) The calculation for the Yibadiao dam has incorporated the dam breach flow of the upper stream Xiaogangjian dam [10].

spreadsheet. Empirical charts to determine the initial tangent m_1 and the asymptote m_2 of the hyperbolic curve were developed based on the unit weight and shear strength parameters of the soil material. The dam breach flood analysis could be performed easily using the spreadsheet DB-IWHR by providing the fifteen input parameters, most of which can be determined based on the experience. The model validation indicated that the differences between the original and the proposed approaches are insignificant in most cases. The proposed simplified method can be useful for the preliminary dam planning and safety review studies. However, detailed analyses based on the laboratory experiments on soil erosion and strength properties along with the successful modeling of lateral enlargement process are still necessary for in-depth study and non-homogeneous dams.

This work was supported by the National Natural Science Foundation of China (Grant No. 41731289), the Foundation of State Key Laboratory of Simulation and Regulation of Water Cycle in River Basin (Grant No. 2016ZY08) and the Consultation and Evaluation Project of the Chinese Academy of Sciences (Grant No. 2018-Z02-A-008).

1 Liu N, Chen Z, Zhang J, et al. Draining the Tangjiashan barrier lake. *J*

- Hydraul Eng*, 2010, 136: 914–923
- Wu W M, Altinakar M S, Al-Riffai M, et al. Earthen embankment breaching. *J Hydraul Eng*, 2011, 137: 1549–1564
 - Singh V P, Scarlatos P D. Analysis of gradual earth-dam failure. *J Hydraul Eng*, 1988, 114: 21–42
 - Fread D L. BREACH: An erosion model for earthen dam failures. National Weather Service (NWS) Report, NOAA. Silver Spring: National Oceanic and Atmospheric Administration, 1988
 - Wu W. Simplified physically based model of earthen embankment breaching. *J Hydraul Eng*, 2013, 139: 837–851
 - Zhang L M, Peng M, Chang D S, et al. Dam Failure Mechanisms and Risk Assessment. London: John Wiley & Sons, 2016. 67–240
 - Chen Z, Ma L, Yu S, et al. Back analysis of the draining process of the Tangjiashan barrier lake. *J Hydraul Eng*, 2015, 141: 05014011
 - Zhou X, Chen Z, Yu S, et al. Risk analysis and emergency actions for Hongshiyuan Barrier Lake. *Nat Hazards*, 2015, 79: 1933–1959
 - Wang L, Chen Z, Wang N, et al. Modeling lateral enlargement in dam breaches using slope stability analysis based on circular slip mode. *EngGeol*, 2016, 209: 70–81
 - Chen S, Chen Z, Tao R, et al. Emergency response and back analysis of the failures of earthquake triggered cascade landslide dams on the Mianyuan River, China. *Nat Hazards Rev*, 2018, 19: 05018005
 - Osman A M, Thorne C R. Riverbank stability analysis. I: Theory. *J Hydraul Eng*, 1988, 114: 134–150
 - Wang L. Study on mechanism of Barrier Lake breaches (in Chinese). Dissertation of Doctoral Degree. Xi'an: Xi'an Polytechnic University, 2017
 - Duncan J M. State of the art: Limit equilibrium and finite element analysis of slopes. *J Geotech Eng*, 1996, 123: 577–596

- 14 Chen Z Y, Shao C M. Evaluation of minimum factor of safety in slope stability analysis. *Can Geotech J*, 1988, 25: 735–748
- 15 Jack R. The mechanics of embankment failure due to overtopping flow. Dissertation of Masteral Degree. Auckland: University of Auckland, 1996
- 16 Zhong Q, Wu W. Discussion of “back analysis of the draining process of the Tangjiashan Barrier Lake” by Zuyu Chen, Liqiu Ma, Shu Yu, Shujing Chen, Xingbo Zhou, Ping Sun, and Xu Li. *J Hydraul Eng*, 2016, 142: 07016001
- 17 Briaud J L. Case histories in soil and rock erosion: Woodrow Wilson Bridge, Brazos River Meander, Normandy Cliffs, and New Orleans Levees. *J Geotech Geoenviron Eng*, 2008, 134: 1425–1447
- 18 Bishop A W. The use of the slip circle in the stability analysis of slopes. *Geotechnique*, 1955, 5: 7–17
- 19 Ru N H, Niu Y G. Embankment dam incidents and safety of large dams (in Chinese). Beijing: China Waterpower Press, 2001. 47–69
- 20 Zhong Q, Chen S, Deng Z. A simplified physically-based model for core dam overtopping breach. *Eng Failure Anal*, 2018, 90: 141–155